Stochastic cloning of dynamical systems with hidden variables

Andrey V. Andreev [1], Alexander N. Pisarchik [2], Nikita Kulagin [1], Rider Jaimes-Reátegui [3], Guillermo Huerta-Cuellar [3], Artem A. Badarin [1], and Alexander E. Hramov [1,*]

[1]*Baltic Center for Neurotechnology and Artificial Intelligence, Immanuel Kant Baltic Federal University, Kaliningrad 236041, Russia*
[2]*Center for Biomedical Technology, Universidad Politécnica de Madrid, Campus Montegancedo, Pozuelo de Alarcón, Madrid 28223, Spain*
[3]*Centro Universitario de Los Lagos, Universdad de Guadalajara, Lagos de Moreno 47463, Mexico*

(Received 7 February 2025; accepted 30 June 2025; published 18 July 2025)

We present an approach combining reservoir computing and nonlinear dynamics to replicate the behavior of stochastic systems, even when only partial observations are available. Unlike conventional RC applications, our approach systematically evaluates the conditions under which a system can be "strongly" cloned (exact trajectory prediction) versus "weakly" cloned (statistical replication), leveraging external noise excitation to infer hidden dynamics. By applying external noise and analyzing the system response, we demonstrate the feasibility of our approach both theoretically and experimentally. We show that strong cloning is achievable only when a deterministic functional relationship exists between the external noise and the system's response. Using the FitzHugh-Nagumo neuron model and a diode-pumped erbium-doped fiber laser as test cases, we show that a "strong" clone—capable of accurately predicting system dynamics—can be constructed for the neuron model, whereas only a "weak" clone, capable of statistical prediction, is achievable for the laser system. These findings underscore the potential of leveraging machine learning and nonlinear dynamics for system identification and prediction in complex real-world scenarios.

DOI: 10.1103/dynj-xqrm

I. INTRODUCTION

The study of dynamical systems is central to statistical and nonlinear physics, but this often faces challenges due to incomplete knowledge of system dynamics. In many cases, only time series data from a single observable are available, limiting traditional approaches like phase space reconstruction [1,2]. Machine learning, particularly reservoir computing (RC), has emerged as a powerful tool for modeling such systems, demonstrating success in reconstructing hidden variables and predicting complex dynamics [3–7]. Its fixed, randomized reservoir structure provides a surprisingly effective trade-off between simplicity and performance, making it a preferred choice in many engineering and scientific applications. However, model reconstruction remains difficult when crucial variables are unobserved.

In this work, we introduce an approach that integrates machine learning with nonlinear dynamics to construct a digital clone of a stochastic system in the absence of explicit equations. We consider dynamical systems that are "silent" in the absence of external stimulation, exhibiting no autonomous dynamics. These systems, treated as "black boxes" with no prior information available, can only be characterized by observing their responses to external stimuli. Our objective is to construct a model that accurately replicates the input-output behavior of the original system, relying solely on the applied external stimulus and the corresponding system response, "without" the knowledge of the internal state variable. To this end, we employ broadband noise as the external stimulus. The rich temporal structure of noise allows us to explore a wide range of input sequences, facilitating the creation of a robust and generalizable model. Then, using only the applied noise and the system response, we can train an RC model to reproduce the system's dynamics and create its clone.

Our approach departs from the traditional RC task of learning full-state dynamics prediction. Instead, we train the RC model using external noise as input and a single, observable variable as the corresponding output. This allows the RC to learn an effective representation of the system input-output mapping, specifically the functional relationship between the applied noise and the observed response. Critically, this learning mapping implicitly captures the influence of the unobserved (hidden) variables on the observed dynamics. The RC model has no explicit knowledge of these hidden variables and does not attempt to identify them directly. However, it can efficiently approximate the system's overall behavior by implicitly representing the hidden variable dynamics within its high-dimensional reservoir space. While noise is conventionally used in RC to mitigate overfitting [8,9], we utilize external noise as a controlled input to actively probe the system dynamics. By analyzing the system response to this stochastic excitation, we effectively capture the influence of the original system's hidden variables on its observable behavior.

We distinguish between two types of cloning as follows [10]. The strong cloning is the reproduction of the exact trajectory of the stochastic system's dynamics over the temporal interval $[0, L\Delta t]$:

$$\max_{t=0,\Delta t,\ldots,L\Delta t} \mathbb{E}(|x_t - r_t|) \leqslant \epsilon, \tag{1}$$

where r_t is the process predicted by the RC model, x_t is the true target process determined by the cloned stochastic

*Contact author: hramovae@gmail.com

 ©2025 American Physical Society

system, $\mathbb{E}(\cdot)$ is the expected value, and ϵ denotes the prediction accuracy—a small value that determines the quality of a strong cloning. The weak cloning is the statistical reproduction with low error between distributions of the important statistical metrics of the predicted and true trajectories, which does not require prediction of the exact trajectory (statistical prediction). In other words, the weak cloning gives a probabilistic model if the condition

$$\max_{t=0,\Delta t,\ldots,L\Delta t} |\mathbb{E}(z(x_t)) - \mathbb{E}(z(r_t))| \leqslant \epsilon \tag{2}$$

is fulfilled for all polynomials $z(\cdot)$. In this case, all moments of the distribution of stochastic processes x_t and r_t turn out to be the same with a given accuracy ε.

In this work, we consider two systems: the stochastic FitzHugh-Nagumo (SFHN) neural model, and the numerical model and experimental setup of the stochastic erbium-doped fiber laser (SEDFL). For both of them, an important statistical metric is the interspike activation interval (ISAI), which is used as a criterion for weak cloning as suggested in the Ref. [10].

Moreover, we analyze the theoretical feasibility of constructing a strong clone for an unknown system subject to external influences. Our analysis confirms that the existence of a deterministic mapping from the external noise to the system's evolution is a necessary condition for strong predictability and, by extension, strong cloning. When such a mapping is absent, any model, even a highly expressive one, can reproduce only the system's statistical behavior.

To enhance the efficiency and fidelity of our approach under partial observability, we explore input optimization strategies. Specifically, we employ delay-coordinate embedding to reconstruct a higher-dimensional phase space, thereby enriching the available information from observed variables. This embedding improves the reservoir's ability to infer hidden dynamics and capture relevant features for prediction and cloning.

II. STOCHASTIC CLONING

A detailed schematic of the proposed approach, based on the RC architecture, is presented in Fig. 1. The RC consists of three layers: an input layer, a hidden reservoir layer, and an output layer. The system is stimulated by an external digital noise signal at discrete time steps $t = j\tau$, where τ is the sampling interval and j denotes the discrete time index. Simultaneously, the system response to this excitation is recorded at the same time instances, providing the necessary data for training and prediction.

The input vector $\mathbf{g}_t$ fed into the input layer of the reservoir is defined as

$$\mathbf{g}_t = (\xi_t, x_t, \xi_{t-\tau}, x_{t-\tau}, \ldots, \xi_{t-n\tau}, x_{t-n\tau})^T. \tag{3}$$

Here, ξ_t represents the external noise applied to the dynamical system, while x_t is the recorded system response. The input vector includes n delayed pairs $(\xi_{t-i\tau}, x_{t-i\tau})$ for $i = 1, 2, \ldots, n$.

Each input signal is weighted by the corresponding coefficients of the input-to-hidden adjacency matrix $\mathbf{W}_{\mathrm{HH}}$ and then passed to the hidden layer, which consists of N_{H} artificial

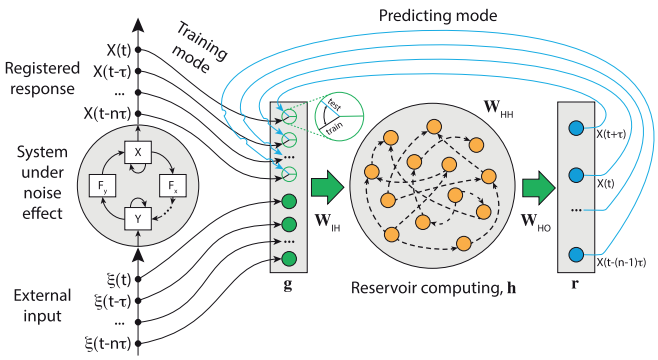

FIG. 1. General scheme for RC training and prediction of stochastic system dynamics. The left part illustrates the excitation of a dynamical system by an external signal and the point-by-point recording of its response. The system may consist of multiple variables; however, in the general case, the input is applied to one variable while another variable is recorded, with all other variables remaining unobserved. The right part depicts the RC training and prediction processes. During training, both the external input signal and the corresponding system response are fed into the RC model. Once training is complete, the RC output replaces the recorded response as input, enabling autonomous prediction of system dynamics. Additionally, incorporating delayed signals as input can enhance prediction accuracy.

neurons. The hidden state dynamics at discrete time steps t follow:

$$\mathbf{h}_t = \tanh(\mathbf{W}_{\mathrm{HH}}\mathbf{h}_{t-\tau} + \mathbf{W}_{\mathrm{IH}}\mathbf{g}_t), \tag{4}$$

where $\mathbf{h}_t$ is a column vector representing the internal hidden state at time t, encoding temporal dependencies from past states and input signals. The reservoir layer is structured as a random network, defined by an adjacency matrix $\mathbf{W}_{\mathrm{HH}} = N_{\mathrm{H}} \times N_{\mathrm{H}}$ with an average node degree $\bar{k}$ and a spectral radius λ (the largest absolute eigenvalue of $\mathbf{W}_{\mathrm{HH}}$). The input-to-hidden adjacency matrix $\mathbf{W}_{\mathrm{IH}}$ is of size $(2n) \times N_{\mathrm{H}}$ and determines the random couplings between input signals and hidden neurons. Following the methodology in [11], each hidden neuron is connected to only one input neuron, ensuring an even distribution where each input variable is assigned to $N_{\mathrm{H}}/(2n)$ neurons. The elements of $\mathbf{W}_{\mathrm{IH}}$ are drawn randomly from a uniform distribution in the range $[-1, 1]$.

The signals from all hidden neurons are passed to the output layer, where each neuron applies a linear regression operation:

$$\mathbf{r}_{t+\tau} = \mathbf{W}_{\mathrm{HO}}\hat{\mathbf{h}}_t, \tag{5}$$

where $\hat{\mathbf{h}}$ represents the augmented reservoir state, an N_{H}-component column vector. Following [12], the components of $\hat{\mathbf{h}}$ are defined as: $\hat{h}_{i,t} = \hat{h}_{i,t}$ if i is odd, and $\hat{h}_{i,t} = \hat{h}^2_{i,t}$ is i is even, $i = 1, \ldots, N_{\mathrm{H}}$. This transformation introduces additional nonlinearity to enhance the predictive capability of the model.

The training process aims to optimize the output weight matrix $\mathbf{W}_{\mathrm{HO}}$ by minimizing the discrepancy between the predicted output $\mathbf{r}_{t+\tau}$ and the target signal $\mathbf{X}_{t+\tau} = \{x_{t+\tau}, x_t, \ldots, x_{t-(n-1)\tau}\}$. To achieve this, we use Tikhonov

regularization to minimize the L_2-error:

$$L_2 = \sum_{t=1}^{T_{\text{train}}} ||\mathbf{r}_{t+\tau} - \mathbf{X}_{t+\tau}||^2 + \beta||\mathbf{W}_{\text{HO}}||^2, \tag{6}$$

where $\beta = 10^{-4}$ is the regularization parameter, and T_{train} denotes the length of the training dataset $\mathbf{g}$. The regularization term $\beta||\mathbf{W}_{\text{HO}}||^2$ prevents overfitting by constraining the magnitude of the weight values.

After training, the RC transitions to the prediction mode. At each time step, a new input vector $\mathbf{g}_{t+\tau}$ is constructed using the previously predicted output $\mathbf{r}_{t+\tau}$ and the externally provided noise value $\xi_{t+\tau}$:

$$\mathbf{g}_{t+\tau} = (\xi_{t+\tau}, r_{t+\tau}, \xi_t, r_t, \ldots, \xi_{t-(n-1)\tau}, r_{t-(n-1)\tau})^T. \tag{7}$$

This vector is then fed into the input layer of the RC, enabling the system to recursively generate future predictions. The process is iterated to obtain the desired number of predicted values, where the predicted system response is given by $x_t = r_t$.

To optimize the performance of the RC model, we employ a grid search method to fine-tune its hyperparameters. Specifically, we explore the following parameter ranges: the average node degree $\bar{k} \in [10, 20]$ and the spectral radius $\lambda \in [0.1, 1.9]$. These parameters play a crucial role in shaping the reservoir dynamics and its ability to effectively learn and reproduce the system behavior [13,14]. For each combination of $\bar{k}$ and λ, we train the RC model and assess its performance in the testing phase, using prediction accuracy as the evaluation metric. The model that demonstrates the highest accuracy in reproducing the system dynamics is selected as the optimal configuration. This resulting RC model serves as a "clone" of the original system, enabling accurate predictions of its behavior under various external influences and providing a valuable tool for further analysis and exploration.

III. CLONING OF STOCHASTIC FITZHUGH-NAGUMO NEURON

To validate the effectiveness of the proposed approach, we apply it to two model systems and one experimental dataset. The first system under investigation is the SFHN neural model, governed by the following set of stochastic differential equations:

$$\begin{aligned} \dot{x} &= x - x^3/3 - y + 0.3, \\ \dot{y} &= 0.08(x - 0.8y + 0.7) + D\xi(t). \end{aligned} \tag{8}$$

Here, x represents the excitatory variable (membrane potential), while y corresponds to the recovery variable. The term $\xi(t)$ denotes zero-mean white Gaussian noise with an autocorrelation function $\langle \xi(t)\xi(t+t_0)\rangle = \delta(t_0)$, and $D = 0.2$ is the noise amplitude. The stochastic system in Eq. (8) is solved using Euler–Maruyama method with a time step of $\Delta t = 0.1$.

The FitzHugh-Nagumo model is a key framework for studying excitable systems, with its stochastic variant capturing noise-driven neuronal dynamics [15,16]. Stochastic forcing reveals the interplay between deterministic behavior and random fluctuations, crucial for real-world systems [17]. Applying our RC-based approach, we demonstrate its ability to replicate SFHN dynamics without full knowledge of internal variables, showcasing its robustness in modeling stochastic systems. In this study, only the external noise $\xi(t)$ and membrane potential $x(t)$ are available, while the recovery variable y remains unobserved. Since $\xi(t)$ directly influences y, the RC model must infer hidden dynamics solely from $x(t)$ and $\xi(t)$, making this a stringent test of its predictive capability.

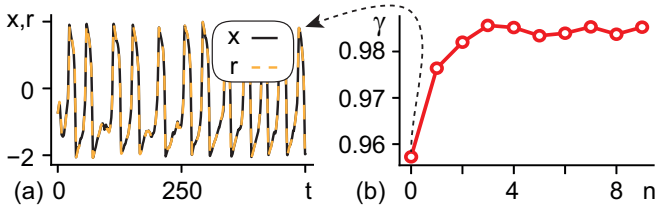

FIG. 2. Results of SFHN system cloning. (a) Times series of x variable (black) and the reconstructed signal r (blue) generated by the RC when driven by the same external noise, shown for $n = 0$ (without delay embeddings). (b) Dependence of the strong prediction accuracy γ on the number of delays n, illustrating the impact of incorporating delayed signals on the predictive performance of the RC model.

To assess the performance of the RC-based approach, we employ a training dataset containing $T_{\text{train}} = 10^5$ samples and a separate testing dataset of $T_{\text{test}} = 10^5$ samples. The hidden reservoir layer comprises $N_{\text{H}} = 2000$ neurons, ensuring sufficient capacity to capture the system dynamics. The time step τ employed for data generation within the reservoir is set equal to the integration step Δt used for solving the stochastic system in Eq. (8).

The accuracy of the RC model is quantified using the metric $\gamma = 1 - \text{NRMSE}$. Here, NRMSE is the normalized root mean square error defined as:

$$\text{NRMSE} = \frac{\sqrt{\frac{1}{T_{\text{test}}}\sum_{t=1}^{T_{\text{test}}}(r_{1,t} - x_t)^2}}{x_{\max} - x_{\min}}, \tag{9}$$

where r_1 represents the predicted signal, x is the true signal, and $x_{\max}$ and $x_{\min}$ are the the maximum and minimum values of the true signal, respectively. A value $\gamma \approx 1$ indicates high prediction accuracy, signifying that the RC model closely replicates the system dynamics. Conversely, $\gamma \approx 0$ suggests poor prediction capability. We define *strong prediction* as an accurate reproduction of the system trajectory, i.e., $\forall t : |r_{1,t} - x_t|| \approx 0$. An RC model capable of such precise replication is referred to as a *strong clone*.

Through hyperparameter optimization, we identified the optimal configuration for the hidden layer as $\bar{k} = 18$ and $\lambda = 0.7$, which resulted in a prediction accuracy of $\gamma = 0.957$. Figure 2(a) illustrates the close agreement between the original SFHN signal x and the RC-predicted signal r. The two signals are nearly indistinguishable, with minor discrepancies primarily occurring during spike generation events.

To further enhance prediction accuracy, we incorporated delayed signals into the input, following the approach described earlier and depicted in Fig. 1. The time delay was set to $\tau = \Delta t$ (one integration step), while the number of delays n was varied. Increasing n up to 3 resulted in a slight improvement in prediction accuracy ($\gamma = 0.986$), whereas a

further increase in n did not yield additional gains. Thus, the RC model with $n = 3$ delayed signals achieves the most accurate cloning of the SFHN neuron, effectively capturing its dynamics with high precision.

The slight decline in weak cloning accuracy for larger n [Fig. 2(c)] may arise from interference between the reservoir's intrinsic memory and excessive input history. While longer contexts provide more data, they can also introduce noise or redundant information that disrupts the reservoir's dynamics. Also, the structure of the input connections is such that each hidden neuron is connected to only one input neuron, ensuring an even distribution where each input variable is assigned to $N_H/(2n)$ neurons. So, increasing n leads to a decrease in the number of connections from each input neuron. The last can negatively influence on the RC's performance.

These findings highlight the effectiveness of the proposed RC-based approach in accurately modeling and predicting the behavior of complex stochastic systems, even in the absence of complete system information. The inclusion of delayed signals significantly enhances the model's ability to capture temporal dependencies, reinforcing its potential as a powerful tool for studying and forecasting the dynamics of excitable systems.

IV. CLONING OF STOCHASTIC DIODE-PUMPED ERBIUM-DOPED FIBER LASER

Another physical system that, like the SFHN neuron, operates in a subthreshold regime in the absence of external influence is a SEDFL modeled by the following dimensionless stochastic equations [18]:

$$\dot{x} = axy - bx + c(y + \upsilon),$$
$$\dot{y} = -dxy - (y + \upsilon) + P_p\left\{1 - \exp\left[-18\left(1 - \frac{y + \upsilon}{\rho}\right)\right]\right\}, \tag{10}$$

where x and y represent the laser intensity and population inversion, respectively. The pump parameter is given by $P_p = P_{p0}(1 + D\xi(t))$, where $P_{p0} = 506$ is the unmodulated pump power ($D = 0$), $\xi(t)$ is a uniform distributed random signal within the range $[-1, 1]$, and $D = 1$ denotes the noise amplitude. The parameters are set as $a = 6.6207 \times 10^7$, $b = 7.4151 \times 10^6$, $c = 0.0163$, $d = 4.0763 \times 10^3$, $\upsilon = 0.3075$ and $\rho = 0.6150$ [19]. The stochastic differential equations are numerically integrated using the Euler–Maruyama method with a time step of $\Delta t = 10^{-7}$.

In experimental studies of the EDFL, only the laser intensity can be directly measured. Consequently, similar to the SFHN case, we use only the external noise $\xi(t)$ and the recorded laser intensity $x(t)$ as inputs to the RC model, while treating the population inversion $y(t)$ as an unobservable variable. For both training and testing, we utilize datasets consisting $T_{\text{train}} = T_{\text{test}} = 10^5$ data points to ensure model performance evaluation.

Achieving a strong clone for the SEDFL system is not feasible. As shown in Fig. 3(a), with no delays ($n = 0$), the predicted variable loosely follows the true dynamics, yielding an accuracy of $\gamma = 0.807$. Varying the delay number n [Fig. 3(c)] improves accuracy slightly, peaking at $\gamma = 0.836$ for $n = 2$, indicating that while some system behavior is captured, precise trajectory replication remains out of reach.

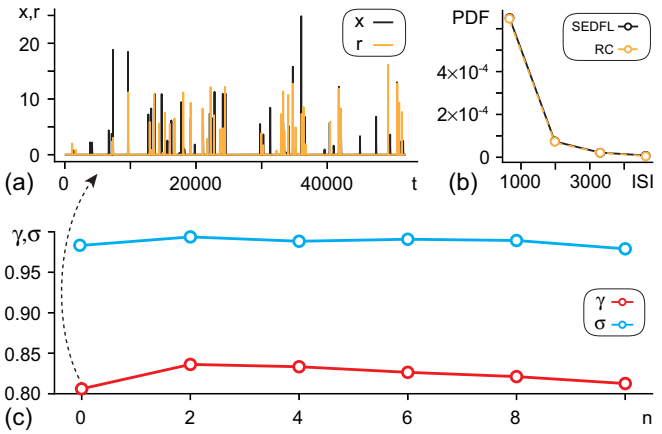

FIG. 3. Results of the SEDFL model cloning. (a) Times series of the laser intensity x (black) and the RC-predicted signal r (blue), both driven by the same external noise, for $n = 0$ (without delays). (b) Probability density functions (PDFs) of the interspike activation intervals (ISAIs) for the original and predicted signals. (c) Dependence of the strong (γ) and weak (σ) prediction accuracy on the number of delayed signals n.

Given this limitation, we focus on statistical characterization, resulting in *weak prediction*. The SEDFL system has a constant background signal and random spiking-like activations, with the latter being our primary interest. To assess weak prediction, we compare ISAIs distributions. As shown in Fig. 3(b), the predicted and true ISAIs closely match, demonstrating that the RC model effectively captures the system's statistical properties despite its limited trajectory accuracy.

To quantify the accuracy of weak prediction, we define the following metric:

$$\sigma = 1 - \frac{\int |\text{PDF}_{\text{SEDFL}} - \text{PDF}_{\text{RC}}|}{\int \text{PDF}_{\text{SEDFL}}}, \tag{11}$$

where $\text{PDF}_{\text{SEDFL}}$ and PDF_{RC} represent the probability density functions of the ISAIs for the original SEDFL system and the RC-predicted signal, respectively. The measure σ evaluates the statistical similarity between these distributions, with values closer to 1 indicating a higher degree of alignment.

Figure 3(c) illustrates the dependence of weak prediction accuracy σ on the number of delays n. The results indicate that σ remains nearly constant across different values of n, ranging from a minimum of $\sigma = 0.979$ at $n = 10$ to a maximum of $\sigma = 0.994$ at $n = 2$. Notably, even without incorporating delayed signals ($n = 0$), the RC model is capable of forming a weak clone of the SEDFL system. While the original and predicted signals do not exhibit a perfect match [Fig. 3(a)], their statistical characteristics–such as the ISAI distributions–are closely aligned [Fig. 3(b)].

V. THEORETICAL ANALYSIS OF THE POSSIBILITY OF CREATING A STRONG CLONE

A crucial question arises: Why are we unable to create a strong clone for the SEDFL model? Is this limitation due to the insufficient capacity of the machine learning model,

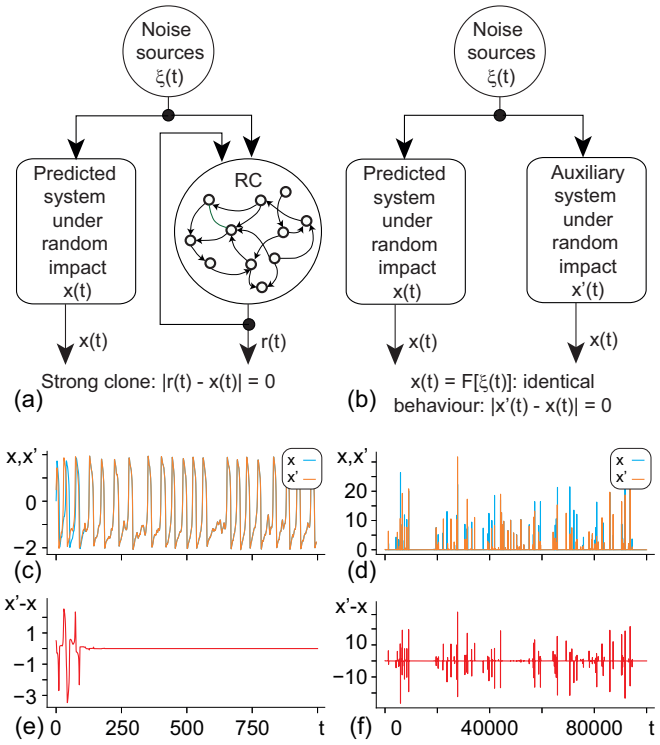

FIG. 4. Construction of strong prediction and strong clone. (a) Prediction using an RC trained on system and noise data. Both the system and RC receive the same noise input $\xi(t)$, enabling trajectory comparison. Strong prediction gives an accurate reproduction of the system trajectory, i.e. $x(t) \approx r(t)$; weak prediction captures only statistical properties. (b) Auxiliary system approach to assess strong cloning. The studied system and an identical auxiliary system with different initial conditions converge if functional dependence exists. (c,d) Time series $x(t)$ and $x'(t)$ for (**c**) SFHN neurons and (d) SEDFL systems with different initial conditions. (e), (f) Differences $(x' - x)$. FHN neurons achieve strong cloning (trajectories match post-transient) (e), while SEDFL systems do not show functional dependence show only probabilistic cloning (f), indicating that the cloning remains only probabilistic.

or are we facing fundamental constraints? To answer this, we must analyze the theoretical feasibility of constructing a strong clone for an unknown system (a "black box") under external influence.

In the proposed cloning scheme, an external stochastic signal $\xi(t)$ drives the system dynamics, which are then used to train the RC model. Figure 4(a) illustrates this predictive framework: the same stochastic signal $\xi(t)$ is applied to both the original system (the target system to be cloned) and the trained RC model. If, after a transient period, the RC model perfectly replicates the original system trajectory, then strong prediction has been achieved. This exact replication implies the existence of a functional dependence $x(t) = F[\xi(t)]$, meaning the system response is uniquely determined by the external stochastic input.

To clarify this idea, consider a hypothetical scenario involving two identical dynamical systems. Suppose a functional dependence $x(t) = F[\xi(t)]$ exists. Now, introduce an auxiliary system $x'(t)$, which is identical to the original system but starts from a different initial condition, i.e., $x'(0) \neq x(0)$. If the same stochastic input $\xi(t)$ is applied to both systems [Fig. 4(b)], and a functional dependence $F[\circ]$ truly governs the system response, then after a transient period, both systems will satisfy $x(t) = F[\xi(t)]$ and $x'(t) = F[\xi(t)]$. As a result, their trajectories will become identical, meaning $|x(t) - x'(t)| = 0$. This confirms that strong prediction–and consequently, strong cloning–is possible only if a deterministic functional relationship between $\xi(t)$ and $x(t)$ exists.

If no functional dependence exists, strong prediction is impossible, and only statistical properties can be captured. To test for strong cloning, we use an auxiliary system approach: if two identical systems with different initial conditions, driven by the same input, converge over time, strong cloning is feasible. Otherwise, only weak prediction is possible, as seen in the SEDFL system.

For the SFHN model, strong cloning was achieved due to a clear functional dependence on external noise, enabling precise trajectory prediction. In contrast, the SEDFL system, influenced by additional factors, allowed only weak cloning, accurately reproducing statistical properties like interspike interval distributions. These results distinguish strong prediction, which requires a functional response-external input relationship, from weak prediction, which captures statistical features in systems lacking such dependence.

Our findings on the SEDFL system correlate with the RC studies of chaotic dynamics [4,5,20], where exact long-term prediction is infeasible due to sensitivity to initial conditions. However, our framework generalizes this limitation: even nonchaotic systems without a functional dependence on external noise can only be weakly cloned, as demonstrated by the SEDFL's statistical reproducibility [Fig. 3(b)]. This aligns with the known RC capability to replicate chaotic attractor statistics [5,20] but introduces a broader criterion–functional noise-dependence–to determine whether strong cloning is possible. For the SEDFL, the lack of such dependence [Figs. 4(d) and 4(f)] confines RC to weak cloning, akin to chaotic systems where prediction horizons are bounded by the Lyapunov time [20].

VI. EXPERIMENTAL VERIFICATION

We experimentally validated our approach using SEDFL, where weak cloning captured statistical properties despite noise interference. Figures 5(a) and 5(b) compare the time series and the PDFs of ISAIs for the experimental laser system (see Appendix) and its *weak clone*, respectively. While the weak clone successfully captures key statistical features of the system dynamics, its performance remains suboptimal. We attribute this limitation to unpredictable background noise introduced during the measurement process, which affects both the recorded signal and the accuracy of statistical modeling. The RC model achieved the highest weak prediction accuracy ($\sigma = 0.883$) with $n = 9$ delays, emphasizing the importance of incorporating delayed signals to account for noise and system complexity. This result underscores the potential of weak cloning in analyzing complex stochastic systems.

VII. CONCLUSIONS

Our findings underscore the fundamental distinction between strong and weak prediction in system cloning. Strong

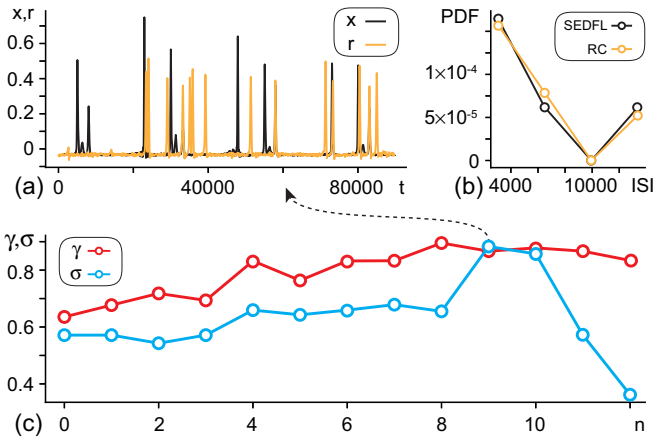

FIG. 5. Results of cloning the experimental SEDFL. (a) Times series of the experimental SEDFL variable x (black) and the reconstructed RC signal r (blue) under the same external stochastic excitation for $n = 9$ delayed signals. (b) Corresponding PDFs of the ISAIs for the experimental system and its RC-based weak clone, demonstrating their statistical similarity. (c) Dependences of strong (γ) and weak (σ) prediction accuracy on the number of the delayed signals n, highlighting the role of delay embedding in improving prediction performance.

prediction is only feasible in systems where a clear functional relationship exists between the response and the external influence. In contrast, weak prediction focuses on replicating statistical properties, providing an alternative method for analyzing stochastic systems that lack functional dependence. By distinguishing between strong and weak predictions, our work advances machine learning-driven modeling of complex stochastic systems with incomplete observability. Future research should explore broader applications and refine RC architectures to enhance weak prediction accuracy, further bridging data-driven modeling with nonlinear dynamics.

ACKNOWLEDGMENT

This work was supported by the Russian Science Foundation (Grant No. 24-71-10072).

DATA AVAILABILITY

The data is not publicly available. The data are available from the authors upon reasonable request.

APPENDIX: EXPERIMENTAL SETUP AND DATA COLLECTION PROCEDURE

We experimentally validated our approach with a noise-driven SEDFL. The schematic of the experimental setup is illustrated in Fig. 6. The laser system consists of a 6.5-m resonator with a 70-cm erbium-doped fiber of a 2.7 μm core diameter. The setup includes a wavelength division multiplexing (WDM) coupler and two fiber Bragg gratings (FBG1 and FBG2, Thorlabs, NJ, USA) with reflectivities of 100% and 95%, respectively, at a central wavelength of 1550 nm. All optical components are built using single-mode fiber (SMF-28, Thorlabs, NJ, USA) with a 200 μm cladding diameter. The SEDFL is pumped by a 977-nm laser diode (LD-BL976PAG500, Thorlabs, NJ, USA), controlled via a polarization controller (PC) and a laser diode controller (LDC-ITC510, Thorlabs, NJ, USA), which also regulates the diode temperature.

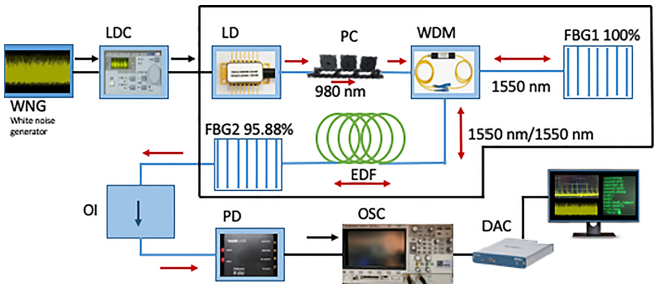

FIG. 6. Schematic of the experimental setup. WNG is a white noise generator, LCD is a laser diode controller, LD is a laser diode, PC is a polarization controller, WDM is a wavelength diffraction modulator, FBG1 and FBG2 are fiber Bragg gratings, EDF is a erbium-doped fiber, OI is an optical isolator, PD is a photodiode, OSC is an oscilloscope, and DAC is a data acquisition controller.

During operation, the diode current is set between 100 mA and 101 mA, just below the EDFL lasing threshold of 105 mA. White noise modulation is applied to the pump current using a waveform generator (WFG-AFG3102, Tektronix, Beaverton, OR, USA). An optical isolator (OI) is incorporated to prevent back reflections into the laser cavity. The optical output from FBG2 is directed to a photodiode (PD2), with signals recorded by an oscilloscope (Agilent DSO-X 3102A) and a data acquisition card (DAC) (NI-BNC-2110). The DAC handles data collection, while the EDFL system temperature is continuously monitored and controlled.

The raw experimental data contained additional noise due to the measurement process, requiring preprocessing to isolate the system response. To remove background noise, we applied a band-pass filter in the frequency range $[0, 0.04]$ Hz. The filtered data were then used to train the RC model on $T_{\text{train}} = 400000$ time points and tested on $T_{\text{test}} = 100000$ points.

[1] M. B. Kennel, R. Brown, and H. D. I. Abarbanel, Determining embedding dimension for phase-space reconstruction using a geometrical construction, Phys. Rev. A **45**, 3403 (1992).

[2] M. Chen, Y. Fang, and X. Zheng, Phase space reconstruction for improving the classification of single-trial EEG, Biomed. Signal Process. Control **11**, 10 (2014).

[3] L. Gonon, L. Grigoryeva, and J.-P. Ortega, Infinite-dimensional reservoir computing, Neural Netw. **179**, 106486 (2024).

[4] Z. Lu, J. Pathak, B. Hunt, M. Girvan, R. Brockett, and E. Ott, Reservoir observers: Model-free inference of unmeasured variables in chaotic systems, Chaos **27**, 041102 (2017).

[5] L.-W. Kong, Y. Weng, B. Glaz, M. Haile, and Y.-C. Lai, Reservoir computing as digital twins for nonlinear dynamical systems, Chaos **33**, 033111 (2023).

[6] A. V. Andreev, A. A. Badarin, V. A. Maximenko, and A. E. Hramov, Forecasting macroscopic dynamics in adaptive Kuramoto network using reservoir computing, Chaos **32**, 103126 (2022).

[7] S. Panahi and Y.-C. Lai, Adaptable reservoir computing: A paradigm for model-free data-driven prediction of critical transitions in nonlinear dynamical systems, Chaos **34**, 051501 (2024).

[8] D. Fry, A. Deshmukh, S. Y.-C. Chen, V. Rastunkov, and V. Markov, Optimizing quantum noise-induced reservoir computing for nonlinear and chaotic time series prediction, Sci. Rep. **13**, 19326 (2023).

[9] A. Wikner, J. Harvey, M. Girvan, B. R. Hunt, A. Pomerance, T. Antonsen, and E. Ott, Stabilizing machine learning prediction of dynamics: Novel noise-inspired regularization tested with reservoir computing, Neural Networks **170**, 94 (2024).

[10] A. E. Hramov, N. Kulagin, A. N. Pisarchik, and A. V. Andreev, Strong and weak prediction of stochastic dynamics using reservoir computing, Chaos **35**, 033140 (2025).

[11] A. E. Hramov, N. Kulagin, A. V. Andreev, and A. N. Pisarchik, Forecasting coherence resonance in a stochastic Fitzhugh–Nagumo neuron model using reservoir computing, Chaos Soliton. Fract. **178**, 114354 (2024).

[12] M. Roy, S. Mandal, C. Hens, A. Prasad, N. Kuznetsov, and M. Dev Shrimali, Model-free prediction of multistability using echo state network, Chaos **32**, 101104 (2022).

[13] H. Jaeger and H. Haas, Harnessing nonlinearity: Predicting chaotic systems and saving energy in wireless communication, Science **304**, 78 (2004).

[14] M. Lukoševičius and H. Jaeger, Reservoir computing approaches to recurrent neural network training, Comput. Sci. Rev. **3**, 127 (2009).

[15] J. Nagumo, S. Arimoto, and S. Yoshizawa, An active pulse transmission line simulating nerve axon, Proc. IRE **50**, 2061 (1962).

[16] A. N. Pisarchik and A. E. Hramov, Coherence resonance in neural networks: Theory and experiments, Phys. Rep. **1000**, 1 (2023).

[17] B. Lindner, J. Garcia-Ojalvo, A. Neiman, and L. Schimansky-Geier, Effects of noise in excitable systems, Phys. Rep. **392**, 321 (2004).

[18] A. N. Pisarchik, A. V. Kir'yanov, Y. O. Barmenkov, and R. Jaimes-Reátegui, Dynamics of an erbium-doped fiber laser with pump modulation: Theory and experiment, J. Opt. Soc. Am. B **22**, 2107 (2005).

[19] J. J. Barba-Franco, L. Romo-Muñoz, R. Jaimes-Reátegui, J. H. García-López, G. Huerta-Cuéllar, and A. N. Pisarchik, Electronic equivalent of a pump-modulated erbium-doped fiber laser, Integration **89**, 106 (2023).

[20] J. Pathak, B. Hunt, M. Girvan, Z. Lu, and E. Ott, Model-free prediction of large spatiotemporally chaotic systems from data: A reservoir computing approach, Phys. Rev. Lett. **120**, 024102 (2018).